Hyper-local to Regional Exposure Contrast of Source-Resolved $PM_{2.5}$ Components across the Contiguous United States: Implications for Health Assessment

Provat K. Saha[1,2], Albert A. Presto[1,2,*], and Allen L. Robinson[1,2,*]

[1]Center for Atmospheric Particle Studies, Carnegie Mellon University, Pittsburgh, Pennsylvania, 15213, USA
[2]Department of Mechanical Engineering, Carnegie Mellon University, Pittsburgh, Pennsylvania, 15213, USA

***Corresponding authors**: Allen L. Robinson and Albert A. Presto; Address: Department of Mechanical Engineering, Carnegie Mellon University, 5000 Forbes Avenue, Pittsburgh, PA 15213, USA; Email: alr@andrew.cmu.edu, apresto@andrew.cmu.edu; Phone: 412-268-3657, 412-721-5203

Abstract:

Background: Improved understanding of what sources and processes drive exposure contrast of fine particulate matter ($PM_{2.5}$) is essential for designing and interpreting epidemiological study outcomes.

Objective: We investigate the contribution of various sources and processes to $PM_{2.5}$ exposure contrasts at different spatial scales across the continental United States.

Methods: We consider three cases: exposure contrast within a metro area, nationwide exposure contrast with high spatial resolution, and nationwide exposure contrast with low spatial resolution. These three cases correspond to common epidemiological study designs. Using high spatial resolution (census-block-level) national empirical model estimates of source- and chemically-specific $PM_{2.5}$ concentration predictions, we quantified the contribution of various sources and processes to $PM_{2.5}$ exposure contrasts in these three cases.

Results: At the metro level (i.e., metropolitan statistical area; MSA), exposure contrasts of $PM_{2.5}$ vary between -1.8 to 1.4 $\mu g\ m^{-3}$ relative to the MSA-mean with about 50% of within-MSA exposure contrast of $PM_{2.5}$ caused by cooking and mobile source primary $PM_{2.5}$. For the national exposure contrast at low-resolution (i.e., using MSA-average mean concentrations), exposure contrasts (relative to the national mean: -3.9 to 3.2 $\mu g\ m^{-3}$) are larger than within an MSA with ~80% of the variation due to secondary $PM_{2.5}$. National exposure contrast at high resolution (census block) has the largest absolute range (relative to the national mean: -4.7 to 3.7 $\mu g\ m^{-3}$) due to both regional and intra-urban contributions; on average, 65% of the national exposure contrast is due to secondary $PM_{2.5}$ with the remaining from the primary $PM_{2.5}$ (cooking and mobile source 26%, other 9%).

Discussion: While national epidemiological studies that use high-spatial-resolution exposure estimates maximizes the exposure contrast of total $PM_{2.5}$, other study designs may offer advantages to investigate health impacts of specific components. City/metro scale studies better isolates the health impacts of primary $PM_{2.5}$ from local sources while national studies with low-spatial resolution can help to infer the health impacts of secondary $PM_{2.5}$.

Keywords: Fine particulate matter, source specific $PM_{2.5}$, exposure contrast

Declaration of competing financial interests: All authors declare they have no actual or potential competing financial interest.

1. Introduction

Airborne fine particulate matter ($PM_{2.5}$; particles with diameter < 2.5 μm) is a complex mixture of chemical species that span a wide range of sizes. $PM_{2.5}$ is directly emitted by sources (primary $PM_{2.5}$) and forms in the atmosphere from oxidation products of precursor gases (secondary $PM_{2.5}$). Numerous epidemiological studies report health risks of $PM_{2.5}$ by comparing spatial patterns in $PM_{2.5}$ exposure with health impacts[1–7]. Although adverse health effects of $PM_{2.5}$ total mass concentration are well established[5], less is known about health risks of size, source, and chemically specific $PM_{2.5}$ components[8–11]. Multiple epidemiological and toxicological studies have investigated the health effects of different sources and chemically specific $PM_{2.5}$ components[8,12–14]. To date, these studies have not revealed consistent results[15].

$PM_{2.5}$ epidemiological studies have been conducted at different spatial scales[5] ranging from a single city[16,17] to national and even continental scales. The spatial scale of exposure estimates used by these studies also varies from relatively low-resolution (average concentrations in cities or metropolitan statistical areas; MSAs)[1,13,18,19] to high-resolution (e.g., zip code level, census tract level) [14,20–22]. City-scale analysis in Los Angeles suggests substantially higher mortality risks than national studies, which suggests that the excess risk is likely associated with the local component of $PM_{2.5}$ exposure[16,17]. The observed health risk in New York City was lower than in Los Angeles, which implies that cities can differ markedly in their local exposure conditions[16].

To estimate the impacts of air pollution on human health, epidemiological studies investigate the correlation of adverse health outcomes with variations in $PM_{2.5}$ concentrations, which are commonly referred to as exposure contrasts. These contrasts are caused by the complex interactions of different sources, processes, and components. For example, primary emissions are responsible for local (e.g., ~100 m – 1 km scale) variations, whereas secondary $PM_{2.5}$ is more regional and therefore creates city-to-city and region-to-region differences[23–26]. Improved quantification of the contribution of different sources and processes to drive exposures at different lengths scales is needed to better design and interpret epidemiological studies.

In this paper, we use national high-spatial-resolution (census block level) predictions of source-specific $PM_{2.5}$ to investigate what sources and components create $PM_{2.5}$ exposure contrasts at different scales and their implications for the design and interpretation of epidemiological studies. We show that cooking and mobile source primary $PM_{2.5}$ are important drivers for intra-urban exposure contrast of total $PM_{2.5}$. At the regional and national scale, secondary $PM_{2.5}$ dominates the total $PM_{2.5}$ exposure contrast. Our analysis provides valuable insights for epidemiological study design focusing on isolating the effects of source- and chemically-specific $PM_{2.5}$ components.

2. Methods

We used national-scale high-spatial-resolution (census block level) empirical models to investigate exposure contrasts of source-specific and total $PM_{2.5}$ mass across the continental US. In this paper we use the term "exposure" to refer to outdoor concentrations. Exposure contrast is defined as the spatial difference in long-term average concentrations. The models are described in section 2.1.

The analysis is performed using predicted concentrations for different geographic units defined by the US Census Bureau. We used the models to predict concentrations at each census block, which is the smallest geographic unit defined by the US Census Bureau. There are ~6 million residential census blocks with a non-zero population in the continental United Sates. In urban areas, census blocks vary in size and shape but typically cover an area of ~0.01 km^2. We also analyzed data for metropolitan statistical areas (MSA), which are centered around a city (minimum population of 50,000) and includes surrounding counties, townships, and suburban areas. There are 363 MSAs in the continental United States.

We consider three cases: (1) exposure contrast within a metropolitan statistical area (MSA) using census block level concentrations, (2) nationwide exposure contrast using MSA-averaged (low spatial resolution) concentrations, and (3) nationwide exposure contrast using census block level (high spatial resolution) concentrations. These three cases correspond to common types of epidemiological studies [5]: single city[16,17], national using low-spatial-resolution exposure data[1,19], and national with high-spatial-resolution exposure data[14,20].

We define exposure contrast within a metropolitan statistical area (MSA) as ($C_{Block} - C_{MSA}$). C_{Block} is the model concentration of total $PM_{2.5}$ or source-specific $PM_{2.5}$ components at a given census block. C_{MSA} is the population-weighted mean concentrations of all block centroids located within an MSA spatial boundary. To quantify national exposure contrast with MSA-average concentrations, we used ($C_{MSA} - C_{National}$), where $C_{National}$ is the population-weighted mean concentration of all census blocks nationwide. To quantify national exposure contrast using census block level concentration data, we used ($C_{Block} - C_{National}$).

2.1 National Estimates of Source-specific $PM_{2.5}$ Components

The analysis focuses on two important urban sources of primary $PM_{2.5}$, traffic and cooking. We also estimate two other categories of $PM_{2.5}$: other primary, and secondary $PM_{2.5}$. Primary $PM_{2.5}$ emissions from traffic or mobile sources is comprised of tailpipe and non-tailpipe emissions. Here we only consider tailpipe emissions, which includes hydrocarbon-like organic aerosol (HOA) and black carbon (BC) particles[27]. Cooking-emitted particles are mostly organic or cooking organic aerosol (COA)[27,28]. We define other primary $PM_{2.5}$ as ($POA_{other} + BC_{other}$), where POA_{other} and BC_{other} are, respectively, primary organic aerosol (POA) and black carbon (BC) particles from other sources. Biomass burning (e.g., wildfires and home heating) is the most important source of other primary $PM_{2.5}$ at a national scale.

We used our published[24] empirical models to predicts national estimates of primary organic aerosol concentrations from emissions for cooking (COA) and mobile sources (HOA) at high spatial resolution. Briefly, the models were derived by performing land use regression (LUR) analysis of High-Resolution Aerosol Mass Spectrometer (HR-AMS) measurements from across the continental US. COA and HOA concentrations were estimated using positive matrix factorization (PMF) of the HR-AMS data using positive matrix factorizatoin[29]. COA and HOA LUR models explain more than 60% of the spatial variability of the measured data ($R^2 = 0.63$ for the COA model and 0.62 for the HOA model). Restaurant density, commercial land use, and urbanicity are the main predictor variables for the COA model. Road density, transportation land use, and urbanicity are the main predictor variables for the HOA model. Saha et al.[24] presents extensive evaluation (e.g., 10-fold cross-validation, a systematic spatial holdout, and comparison

with chemical transport model simulation) to demonstrate model robustness and transferability. We applied the models to predict COA and HOA concentrations at ~6 million residential census blocks with a non-zero population.

BC is another important primary $PM_{2.5}$ component of traffic emissions. Following the approach of Saha et al.[24], we derived a national land-use regression model for BC using a combination of mobile and fixed-site data (details are described in the SI: Section-S1, Fig. S1-S7, Table S1-S3). The data set of measured BC concentrations includes high spatial resolution mobile measurements from three cities (Pittsburgh, PA, Oakland, CA, and Baltimore, MD) and data from the US-EPA's $PM_{2.5}$ speciation networks. These data were fit using the same land use and source activity data set as the COA and HOA models and a supervised linear regression approach based on the ESCAPE protocol[30,31]. The BC LUR model explains about 70% of the spatial variability of the measured data with road density, urbanicity, transportation, and residential land use as the predictor variables (model fit R^2: 0.74; random 10-fold CV R^2: 0.71; systematic spatial holdout R^2: 0.66). Like COA and HOA, the cross-validated BC model was applied to predict the census block-level concentrations across the continental US. Our COA, HOA, and BC estimates are the annual average concentrations in 2017.

Our BC model predicts total BC concentrations. To apportion the predicted BC concentration into mobile (BC_{mobile}) versus other (BC_{other}) sources, we utilized elemental carbon (EC) emission data from mobile versus other sources from National Emission Inventory (NEI, 2017)[32]. Details are described in the SI: Section S2, Figs. S8-S9. Briefly, BC_{other} = BC (county average) × fraction of county-average EC emission from other sources. NEI emission data are aggregated to the county level. Therefore, we used the county average BC concentration to estimate BC_{other} and assign this value to all census blocks within the county boundary. This is reasonable because BC_{other} is dominated by biomass burning (wildfires), which shows smaller variation within a county. We estimated census block level BC from mobile sources as $BC_{mobile} = (BC - BC_{other})$.

HOA and COA are major contributors to POA, especially in urban areas[27,33,34]. However, there are other sources of POA, for instance, biomass burning organic aerosol. We estimated POA from other sources (POA_{other}) as POA_{total} – (HOA+COA). We estimated total POA using the OC/BC ratio technique[35,36] (i.e., $POA_{total} = BC \times [OC/BC]_{primary} \times [OA/OC]_{primary}$ and census block predictions of BC concentrations). We used values for $[OC/BC]_{primary}$ (typical value: 1.7 – 2.0) and $[OA/OC]_{primary}$ (typical value: 1.3 – 1.4) from the literature[37,38] Details are in the SI: section S3 and Fig. S10

Secondary $PM_{2.5}$ is formed via atmospheric chemistry, and includes secondary organic aerosol (SOA), sulfate, nitrate, and ammonium. We estimated the secondary $PM_{2.5}$ in each census block as the total $PM_{2.5}$ minus primary $PM_{2.5}$. The predicted total $PM_{2.5}$ mass concentrations are from the national empirical model of Kim et al[39]. These are census block-level annual-average concentrations in 2015 across the contiguous US, derived from regulatory monitoring, land use characteristics, satellite-based estimates of air pollution, and empirical regression modeling.

The primary $PM_{2.5}$ concentrations discussed above are from combustion sources only. However, there could be non-combustion primary $PM_{2.5}$, such as resuspended road dust, tire, and brake wear particles from mobile sources[40,41]. Since we estimated secondary $PM_{2.5}$ as total $PM_{2.5}$ minus

combustion primary $PM_{2.5}$, these non-combustion primary particles will be part of secondary $PM_{2.5}$ in our analysis. However, their contribution is much lower compared to secondary $PM_{2.5}$ species[40,42].

2.2 Comparison of Source-Specific $PM_{2.5}$ Concentrations Against Chemically Speciated $PM_{2.5}$ Monitoring Data

To assess the robustness of our source- and chemically-specific $PM_{2.5}$ concentration estimates, we compared predicted concentrations to US-EPA's speciated $PM_{2.5}$ monitoring networks data. We used 2015-annual average speciated $PM_{2.5}$ concentrations from 240 monitoring sites across the continental US. This includes sites from both urban (US EPA's Chemical Speciation Network: CSN) and rural (Interagency Monitoring of PROtected Visual Environments: IMPROVE network) locations across the country. The comparisons were made using the predicted concentration estimates at the census-block centroid nearest to each monitoring site. Details are given in the SI: Section S4, Figs. S11-12.

The comparison included (i) predicted primary $PM_{2.5}$ from cooking, mobile, and other sources versus measured primary $PM_{2.5}$ species (EC + POA), (ii) predicted secondary $PM_{2.5}$ (total $PM_{2.5}$ minus primary $PM_{2.5}$) versus measured secondary $PM_{2.5}$ species (SO_4+NO_3+NH_4+SOA), and (iii) predicted total $PM_{2.5}$ versus the sum of speciated measured $PM_{2.5}$ (SO_4, NO_3, NH_4, SOA, POA, and EC). The measured and predicted concentrations agreed within 10-15% in all cases (Fig. S12).

3.0 RESULTS

3.1 National Spatial Variability in Source-specific $PM_{2.5}$ Components

Figure 1 shows the predict source-specific $PM_{2.5}$ concentrations. Fig.1A shows nationwide concentrations of cooking plus mobile source primary $PM_{2.5}$. As expected, primary $PM_{2.5}$ from mobile and cooking sources show substantial spatial variability with hotspots in urban areas and near roadways.

The interquartile range of census-block level concentrations of cooking primary $PM_{2.5}$ is 0.08 – 0.44 (population-weighted national mean: 0.4) $\mu g\ m^{-3}$; for mobile source primary $PM_{2.5}$: 0.14 – 0.57 (0.52) $\mu g\ m^{-3}$, and other primary $PM_{2.5}$: 0.55 – 0.73 (0.71) $\mu g\ m^{-3}$. Other primary $PM_{2.5}$ is relatively less spatially variable than cooking and mobile source primary $PM_{2.5}$ (Fig. 1B). This is expected because biomass burning (a regional source) is likely an important source of other primary $PM_{2.5}$.

As expected, secondary $PM_{2.5}$ is less spatially variable than primary $PM_{2.5}$ (Fig. 1C). The interquartile range of the national secondary $PM_{2.5}$ concentration surface is 5.38 -7.34 $\mu g\ m^{-3}$ (population-weighted national mean 6.37 $\mu g\ m^{-3}$). Secondary $PM_{2.5}$ is the dominant contributor to total $PM_{2.5}$ mass exposure in the US, even in highly populated urban areas. Nationally, ~ 80 % of the national population weighted average total $PM_{2.5}$ mass comes from secondary $PM_{2.5}$. Cooking primary $PM_{2.5}$ contributes 5%, mobile source primary $PM_{2.5}$ contributes 6%, and other primary $PM_{2.5}$ contributes 9%.

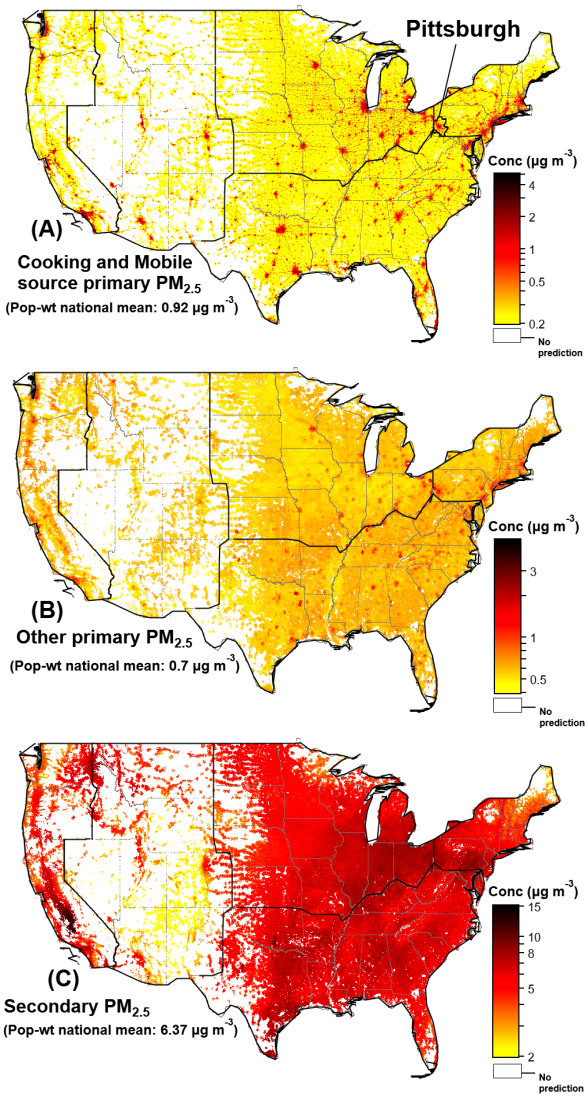

Fig. 1: Census block level concentration estimates of source-specific $PM_{2.5}$ components across the continental US. (A) cooking plus mobile source primary $PM_{2.5}$, (B) other primary $PM_{2.5}$, and (C) secondary concentrations. Color scales are in log-scale and differ across panels.

3.2 Intra-Urban Exposure Contrast

Single-city epidemiological studies depend on intra-urban exposure contrast. To quantify the drivers for intra-urban variability of $PM_{2.5}$, we investigated the spatial variation in source-specific $PM_{2.5}$ within each metropolitan statistical area (MSA) in the continental US. Our analysis reveals that primary $PM_{2.5}$ strongly drives within-MSA exposure contrast of total $PM_{2.5}$ with a major contribution from cooking and mobile source primary $PM_{2.5}$.

To illustrate the spatial pattern of cooking and mobile source primary $PM_{2.5}$ across an MSA, Fig. 2A shows a concentration map for the Pittsburgh MSA. There is substantial within-MSA spatial variability for cooking and mobile primary $PM_{2.5}$. For example, census block level cooking and mobile source primary $PM_{2.5}$ vary by a factor of nine across the Pittsburgh MSA. In contrast, other primary $PM_{2.5}$ vary by a factor of 2.5 and secondary $PM_{2.5}$ by a factor of 1.3.

To further illustrate the variability of source-specific $PM_{2.5}$ components across the Pittsburgh MSA, Fig. 2B shows concentrations along a transect that passes through the central business district. The contribution of cooking and mobile source primary $PM_{2.5}$ to total $PM_{2.5}$ is highest in downtown and gradually decreases as one moves away from the city center (Fig.2B). Although cooking and mobile source primary $PM_{2.5}$ contribute less than 20% of the total $PM_{2.5}$ mass concentrations, they largely drive spatial variability of total $PM_{2.5}$ across the Pittsburgh MSA. Along the transect line, other primary $PM_{2.5}$ is less variable than cooking and mobile source primary $PM_{2.5}$. Whereas secondary $PM_{2.5}$ shows minimal variability.

To quantify what fraction of within-MSA spatial variability of total $PM_{2.5}$ can be explained by the cooking and traffic primary $PM_{2.5}$, we compare the within-MSA spatial variability of census-block level background subtracted $PM_{2.5}$ ($\Delta PM_{2.5}$) versus cooking and mobile source primary $PM_{2.5}$. We defined the $\Delta PM_{2.5}$ as block-level $PM_{2.5}$ minus 5^{th} percentile of block-level $PM_{2.5}$ within the MSA boundary (Fig. 2B). In Pittsburgh MSA, the slope of within-MSA $\Delta PM_{2.5}$ versus cooking and mobile source primary $PM_{2.5}$ regression is ~ 0.51, indicating cooking and source primary $PM_{2.5}$ explain about 50% of within-MSA spatial variability of total $PM_{2.5}$. The remaining variability comes from other primary and secondary $PM_{2.5}$.

While Fig. 2B illustrates the important contribution of primary $PM_{2.5}$ for within-MSA spatial variability, the overall $PM_{2.5}$ mass exposure is dominated by secondary $PM_{2.5}$, even at the city center. We examined the chemical speciation data from an urban background CSN site in Pittsburgh (Lawrenceville, AQS # 42-003-0008; Fig. 2B, right bar plot). Our estimate of secondary $PM_{2.5}$ in Pittsburgh is comparable with the sum of speciated secondary $PM_{2.5}$ measurements (SO_4, NO_3, NH_4, and SOA).

Fig. 2C shows the within-MSA exposure contrast (C_{Block} - C_{MSA}) along the transect line. The exposure contrast for cooking and mobile primary $PM_{2.5}$ and total $PM_{2.5}$ peak in the city center (downtown). The spatial distribution of exposure contrasts for cooking and mobile primary $PM_{2.5}$ versus total $PM_{2.5}$ look similar (Fig. 2C). This implies that these two primary sources are important for the overall exposure contrast for total $PM_{2.5}$ within the MSA. On average, 50% of within-MSA exposure contrast for total $PM_{2.5}$ in Pittsburgh comes from the exposure contrast in cooking and mobile source primary $PM_{2.5}$.

To demonstrate that the results from the Pittsburgh MSA are broadly representative, Fig. 3A-C summarizes the within-MSA exposure contrasts for all MSAs within the continental US (n= 363) rank ordered by MSA population (Fig.3D). Within-MSA exposure contrasts of $PM_{2.5}$ relative to the MSA-mean vary between -1.8 to 1.4 $\mu g\ m^{-3}$. Our analysis indicates that cooking and mobile source primary $PM_{2.5}$ explain between 22% and 94% of within-MSA exposure contrasts of $PM_{2.5}$ across the 363 MSAs (SI: Section S5, Fig. S13). On average they explain 51% with the reminder due to other primary and secondary $PM_{2.5}$.

Our mobile sources primary $PM_{2.5}$ does not account for non-tailpipe primary $PM_{2.5}$, such as traffic-related brake wear, tire wear, and resuspended road dust. These components are lumped within the secondary $PM_{2.5}$ and could contribute to within-MSA exposure contrast. Currently, the relative important of non-tailpipe primary $PM_{2.5}$ is growing[40]. Past studies also reported evidence of an intra-urban gradient of secondary $PM_{2.5}$[34]. Therefore, local secondary $PM_{2.5}$ production can contribute to within-MSA exposure contrast.

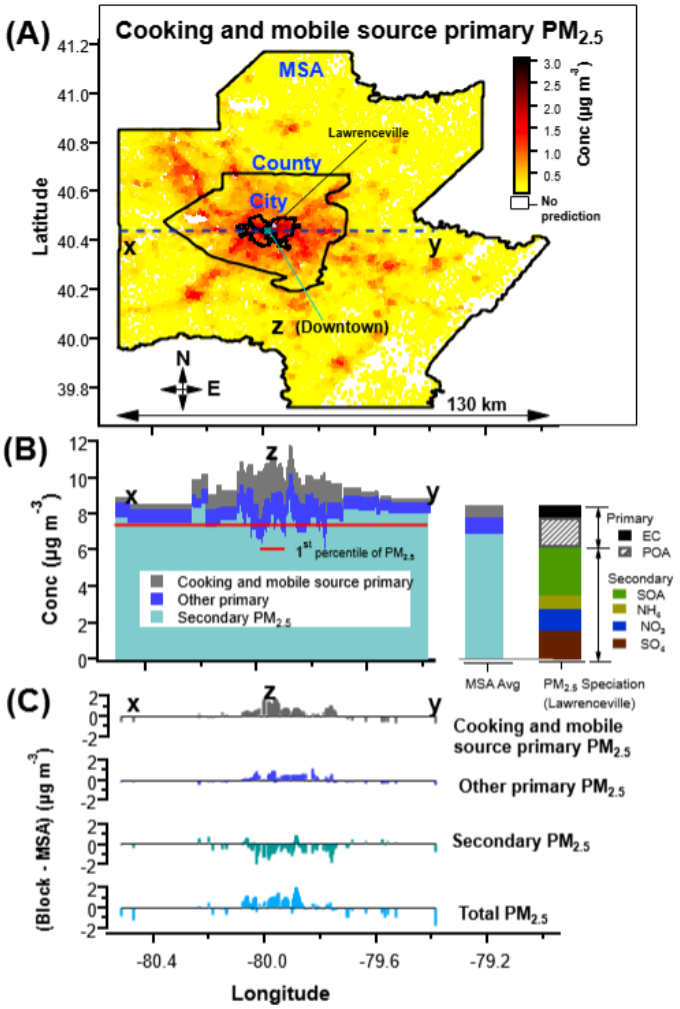

Fig. 2: Exposure contrast within the Pittsburgh Metropolitan Statistical Area (C_{Block} - C_{MSA}). (A) Map showing the distribution of cooking and mobile source primary $PM_{2.5}$ concentrations across the Pittsburgh Metropolitan Statistical Area (MSA). (B) The concentration of source-resolved $PM_{2.5}$ components along a transect line (x-z-y) that passes through the city center (downtown Pittsburgh). The transect line (x-z-y) is shown in Panel-A. The rightmost bar plot on panel-B shows the 2015 annual average chemical composition of $PM_{2.5}$ in Pittsburgh using data from an urban background CSN site in Lawrenceville (AQS#42-003-0008). (C) Exposure contrast (C_{Block} - C_{MSA}) of total and source-specific $PM_{2.5}$ components along the transect line x-z-y.

3.3 National Exposure Contrast with Low Spatial Resolution

National/multi-city epidemiological studies often use low-spatial resolution exposure estimates (e.g., MSA-average, county-average). Our analysis indicates that about 70-90% of between-MSA exposure contrast using MSA-average concentrations is due to secondary $PM_{2.5}$ (Fig. 3F-J). Primary $PM_{2.5}$ contributes little to these between-MSA exposure contrasts. Relative to the national mean, between MSA exposure contrast varies between -3.9 to 3.2 µg m^{-3}. The between MSA exposure contrast is larger than within MSA exposure contrast.

Fig. 4 presents between-MSA exposure contrast for total and source-specific $PM_{2.5}$ components by region. There is substantial variability in MSA-average total $PM_{2.5}$ exposures within and between regions, which are largely due to secondary $PM_{2.5}$ concentrations. Maps in Fig. 4C show the nationwide spatial distribution of between-MSA exposure contrasts for total and source-specific $PM_{2.5}$ components. There are regional hotspots in the Midwest/northeast and the southern US. These are due to inorganic sulfate and nitrate in the Midwest/northeast and (biogenic) secondary organic aerosol in the southeast[43].

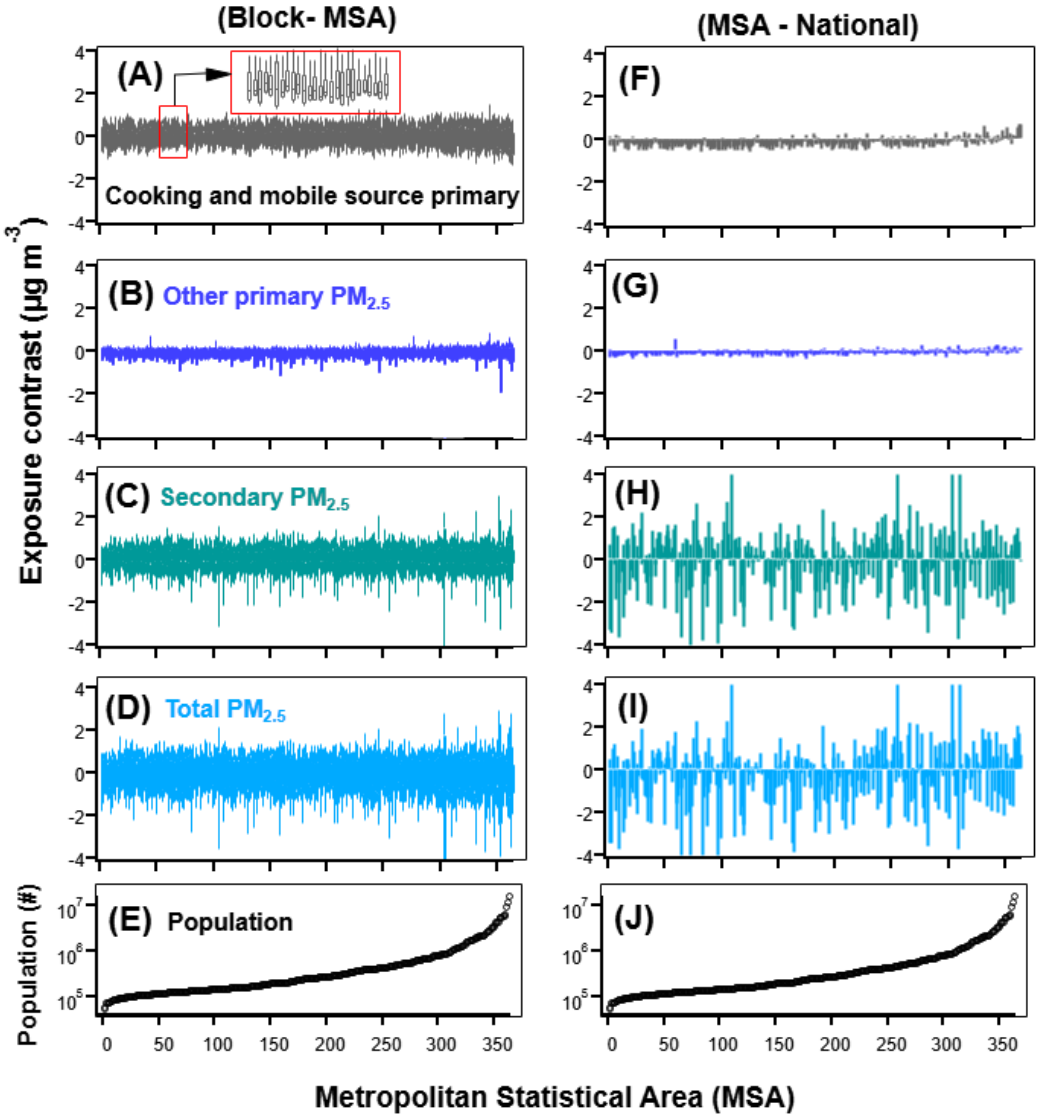

Fig. 3: Within- and between-MSA (Metropolitan Statistical Area) exposure contrasts across the continental US (n= 363). MSAs are ranked by the total MSA population (as shown in panels E and J). (A) Boxplots of within-MSA exposure contrast (C_{Block}- C_{MSA}) for cooking and mobile source primary $PM_{2.5}$ (the inset in panel-A shows the zoom-in view of the small red rectangle area). (B-D) Similar to panel-A, within-MSA exposure contrasts for (B) other primary $PM_{2.5}$, (C) secondary $PM_{2.5}$, and (D) total $PM_{2.5}$. (F-I) Sticks show MSA-average exposure contrast relative to nation mean (C_{MSA}- $C_{National}$); (F) cooking and mobile source primary $PM_{2.5}$, (G) other primary $PM_{2.5}$, (H) secondary $PM_{2.5}$, and (G) total $PM_{2.5}$ (G).

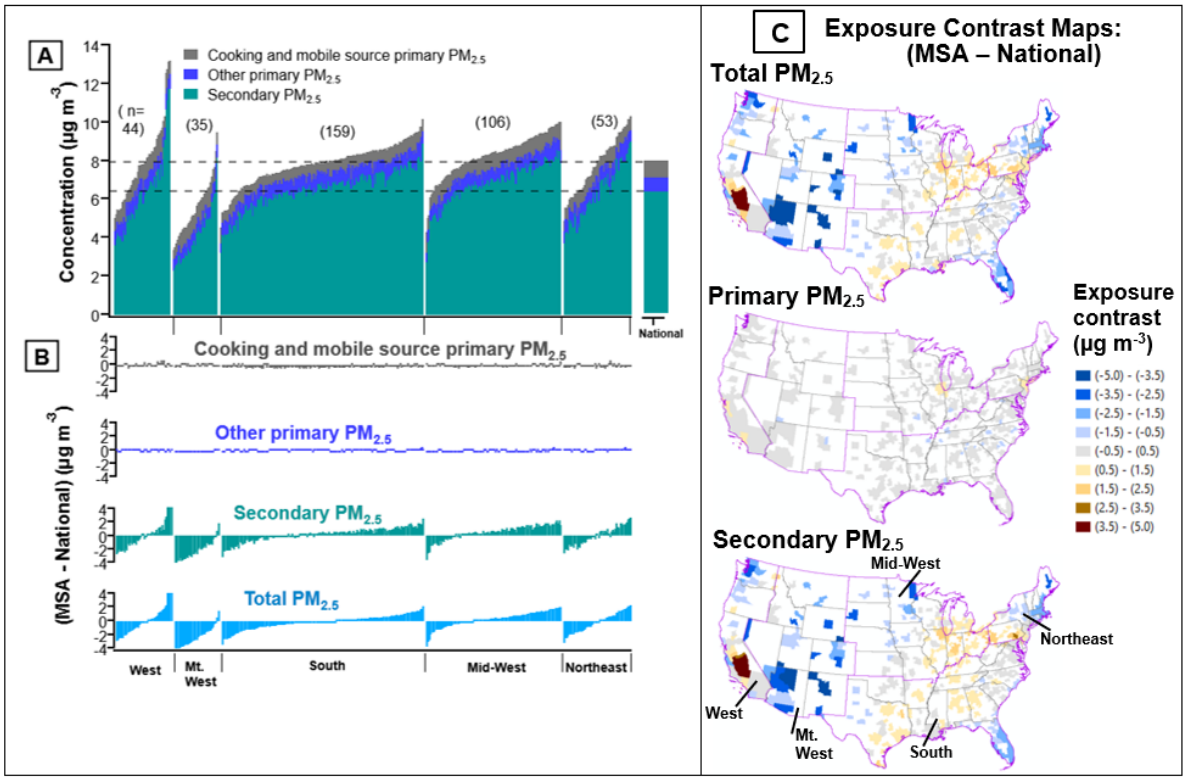

Fig. 4: Exposure contrast between MSA average $PM_{2.5}$ (C_{MSA}- $C_{National}$). (A) Stacked bars of MSA-average concentrations of cooking and mobile source primary $PM_{2.5}$, other primary $PM_{2.5}$, and secondary $PM_{2.5}$. The total height of the bar is the MSA-average total $PM_{2.5}$ concentration. (B) Exposure contrast between MSAs (C_{MSA}- $C_{National}$) for cooking and mobile source primary $PM_{2.5}$, other primary $PM_{2.5}$, secondary $PM_{2.5}$, and total $PM_{2.5}$. (C) Maps of the exposure contrast between MSAs for total $PM_{2.5}$, primary $PM_{2.5}$ (sum of cooking and mobile source primary $PM_{2.5}$ and other primary $PM_{2.5}$), and secondary $PM_{2.5}$. In panels A and B, MSAs are grouped by region (West, Mountain West, South, Midwest, and Northeast) and then rank-ordered within a region by MSA-average total $PM_{2.5}$ concentrations.

3.4 National Exposure Contrast with High Spatial Resolution

In the last decade, researchers have begun used high-spatial-resolution $PM_{2.5}$ estimates for national epidemiology studies[14,20–22]. To better understand the drivers of exposure contrast in these types of studies, Fig.5 presents the nationwide exposure contrast of source-specific $PM_{2.5}$ components using high spatial resolution (census-block-level) concentration estimates (C_{Block} – $C_{National}$).

Compared to intra-urban (Fig. 3) and intra-MSA (Fig. 4), national census block concentrations have the largest absolute variation (relative to the national mean: - 4.7 to 3.7 µg m^{-3}) due to both regional and intra-urban contributions. Fig. 5 indicates that cooking and mobile source primary $PM_{2.5}$ and secondary $PM_{2.5}$ all contribute to total $PM_{2.5}$ exposure contrast. In comparison, other primary $PM_{2.5}$ has a much smaller contribution to exposure contrast.

Hotspots for cooking and traffic primary $PM_{2.5}$ are in cities (Fig. 5A). These hotspots are important contributors to exposure contrast in high-resolution national studies (Fig. 5A), but mostly disappear in a national comparison of MSA average concentrations (see Fig. 4C). High spatial resolution national studies also capture the hotspots of secondary $PM_{2.5}$ (Fig. 5C).

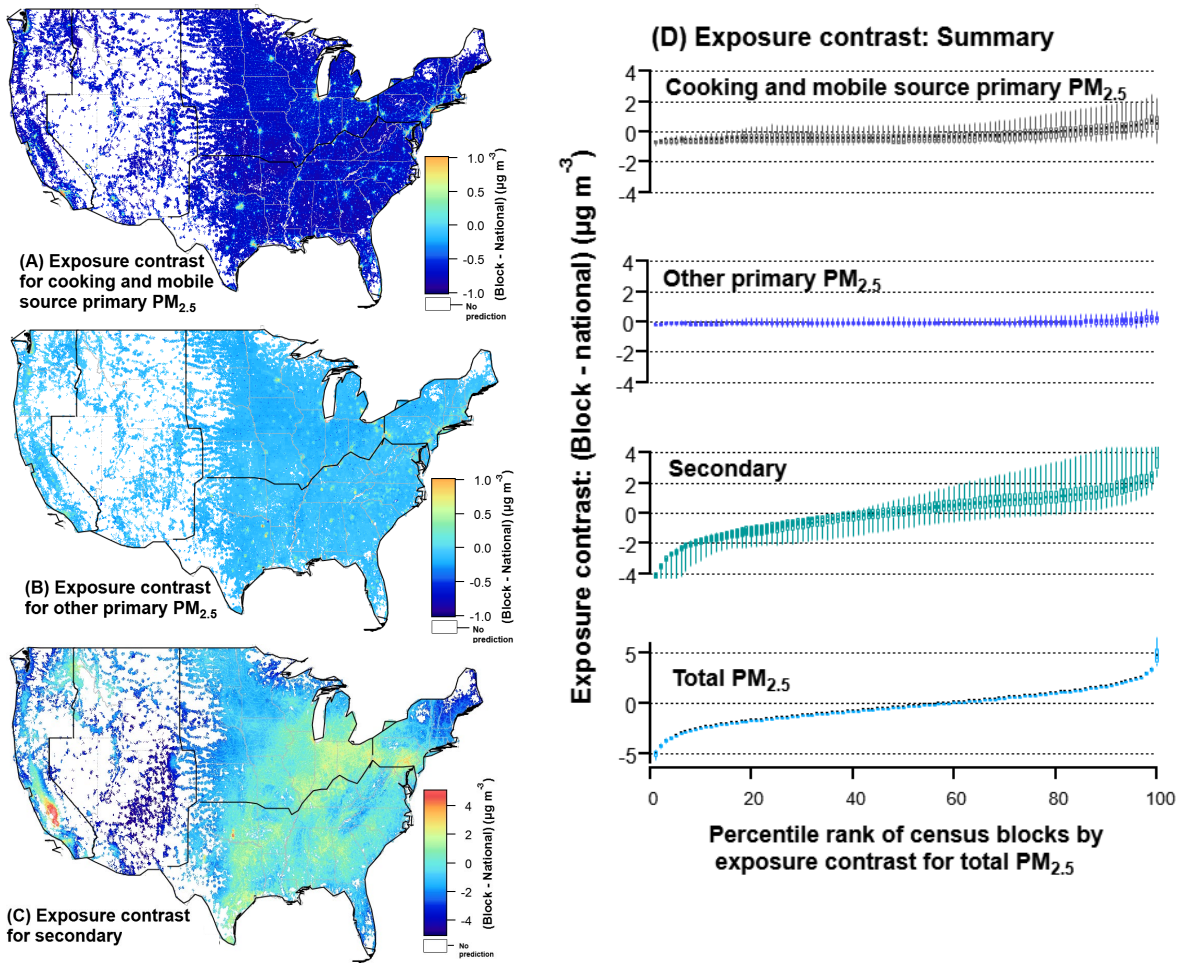

Fig. 5: Census block level exposure contrast ($C_{Block} - C_{National}$) across the continental US. Maps of exposure contrast for (A) cooking and mobile source primary $PM_{2.5}$, (B) other primary $PM_{2.5}$ (B), and (C) secondary $PM_{2.5}$. (D) Census-block-level exposure contrasts for cooking and mobile source primary $PM_{2.5}$, other primary $PM_{2.5}$, secondary $PM_{2.5}$, and total $PM_{2.5}$ rank ordered by total $PM_{2.5}$ exposure contrast and grouped into 100 bins.

Fig.5D summarizes the nationwide census block-level exposure contrast ($C_{Block} - C_{National}$). While secondary $PM_{2.5}$ dominate the total $PM_{2.5}$ exposure contrast across the country, cooking and traffic primary $PM_{2.5}$ are important in certain locations. In addition, the contributions of cooking and traffic primary $PM_{2.5}$ to overall exposure contrast are largest in census blocks with high PM2.5 exposure contrast; these census blocks are typically in urban areas.

We conducted a similar analysis using directly measured speciated $PM_{2.5}$ data from US-EPA's speciated $PM_{2.5}$ monitoring sites across the country (Fig. S14) using 2015-annual average concentrations of major $PM_{2.5}$ species (SO_4, NO_3, NH_4, SOA, POA, EC). Similar to the model-

based results (Fig. 5), the measured composition data indicate that secondary species (SO_4, NO_3, NH_4, SOA) dominate nationwide exposure contrast for total $PM_{2.5}$. However, primary components (EC, POA) have a significant contribution in total $PM_{2.5}$ exposure contrast in many urban locations (Fig.S14).

4. Discussion

Using census-block level concentration estimates, our study provides insight into the drivers of exposure contrast for source-specific $PM_{2.5}$ components across the continental US. Fig. 6 summarizes the results for the three different cases. Since we estimated exposure contrast relative to the national-mean and MSA-mean, it can be positive and negative. Therefore, to compare an average exposure contrast for different spatial scenarios, we calculated the root mean square (RMS) difference, instead of arithmetic mean; specifically, we calculated the RMS of ($C_{Block} - C_{National}$), ($C_{MSA} - C_{National}$) and ($C_{Block} - C_{MSA}$). For the within-MSA case, we used an arithmetic average of RMS ($C_{Block} - C_{MSA}$) across all MSAs. Details on this calculation are given in Table S-4.

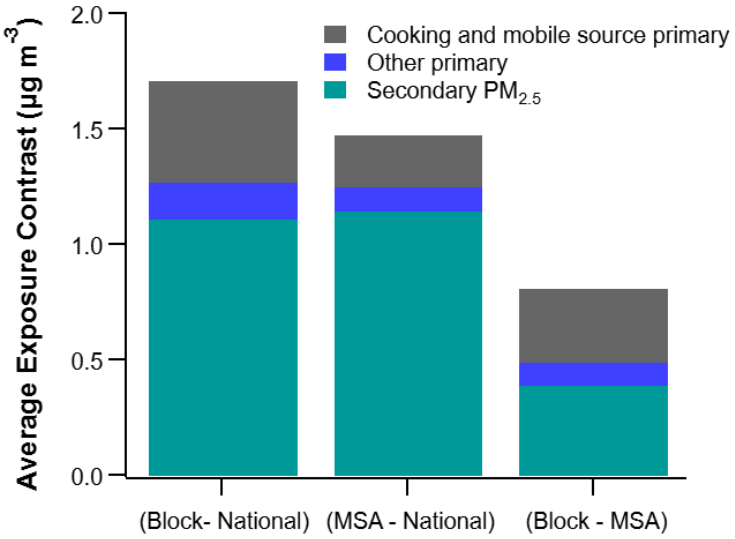

Fig. 6: Contribution of source-specific $PM_{2.5}$ components to average exposure contrast of total $PM_{2.5}$ mass. Bars show the contribution of cooking and traffic primary $PM_{2.5}$, other primary $PM_{2.5}$, and secondary $PM_{2.5}$ to total $PM_{2.5}$ exposure contrast. The full height of each bar indicates exposure contrast for total $PM_{2.5}$.

Fig. 6 indicates that the largest exposure contrast is high resolution national estimate, followed MSA-average and then within-MSA cases. In the national-average of census-block-level exposure contrast ($C_{Block} - C_{National}$), 26% of total $PM_{2.5}$ exposure contrast comes from cooking and mobile source primary $PM_{2.5}$, 9% from other primary $PM_{2.5}$, and 65% from secondary primary $PM_{2.5}$. In national-average of MSA-level exposure contrast of total $PM_{2.5}$, cooking and mobile source primary $PM_{2.5}$ contribute 15%, other primary $PM_{2.5}$ contributes 7%, and secondary $PM_{2.5}$ contributes 78%. For the within-MSA exposure contrast, about 50% of total $PM_{2.5}$ exposure contrast comes from cooking and mobile source primary $PM_{2.5}$.

Our results have implications for the design and interpretation of epidemiological studies investigating the health impacts of $PM_{2.5}$ sources and components. While high spatial resolution national studies provide maximum exposure contrasts, city and MSA-average designs better isolate individual components. MSA-average exposure contrasts are largely driven by secondary $PM_{2.5}$. For example, Fig. 6 indicates that secondary $PM_{2.5}$ contributes about 80% to total $PM_{2.5}$ exposure contrast for exposure contrast estimated using MSA-average concentrations. Therefore, a national-scale epidemiological study using MSA-, or country-average exposure concentrations can help to infer the health impacts of secondary $PM_{2.5}$ while minimizing the influence of primary $PM_{2.5}$. In contrast, city/metro scale epidemiological studies maximize the exposure contrast of primary $PM_{2.5}$. Although primary $PM_{2.5}$ is a relatively minor component of total $PM_{2.5}$ exposure (even at the city center), it drives the majority of the within-MSA exposure contrast of total $PM_{2.5}$. Therefore, a city/metro scale study using high-resolution exposure data may better isolate the health effects of primary sources.

References

(1) Dockery, D. W.; Pope, C. A.; Xu, X.; Spengler, J. D.; Ware, J. H.; Fay, M. E.; Ferris, B. G.; Speizer, F. E. An Association between Air Pollution and Mortality in Six U.S. Cities. *N. Engl. J. Med.* **1993**, *329* (24), 1753–1759. https://doi.org/10.1056/NEJM199312093292401.

(2) Pope III, C. A.; Burnett, R. T.; Thun, M. J.; Calle, E. E.; Krewski, D.; Ito, K.; Thurston, G. D. Lung Cancer, Cardiopulmonary Mortality, and Long-Term Exposure to Fine Particulate Air Pollution. *JAMA* **2002**, *287* (9), 1132–1141. https://doi.org/10.1001/jama.287.9.1132.

(3) III, C. A. P.; Dockery, D. W. Health Effects of Fine Particulate Air Pollution: Lines That Connect. *J. Air Waste Manag. Assoc.* **2006**, *56* (6), 709–742. https://doi.org/10.1080/10473289.2006.10464485.

(4) Pope, C. A.; Ezzati, M.; Dockery, D. W. Fine-Particulate Air Pollution and Life Expectancy in the United States. *N. Engl. J. Med.* **2009**, *360* (4), 376–386. https://doi.org/10.1056/NEJMsa0805646.

(5) Pope, C. A.; Coleman, N.; Pond, Z. A.; Burnett, R. T. Fine Particulate Air Pollution and Human Mortality: 25+ Years of Cohort Studies. *Environ. Res.* **2019**, 108924. https://doi.org/10.1016/j.envres.2019.108924.

(6) Bennett, J. E.; Tamura-Wicks, H.; Parks, R. M.; Burnett, R. T.; Iii, C. A. P.; Bechle, M. J.; Marshall, J. D.; Danaei, G.; Ezzati, M. Particulate Matter Air Pollution and National and County Life Expectancy Loss in the USA: A Spatiotemporal Analysis. *PLOS Med.* **2019**, *16* (7), e1002856. https://doi.org/10.1371/journal.pmed.1002856.

(7) Pope, C. A.; Cohen, A. J.; Burnett, R. T. Cardiovascular Disease and Fine Particulate Matter: Lessons and Limitations of an Integrated Exposure Response Approach. *Circ. Res.* **2018**, *122* (12), 1645–1647. https://doi.org/10.1161/CIRCRESAHA.118.312956.

(8) HEI. *Understanding the Health Effects of Components of the Particulate Matter Mix: Progress and Next Steps*. Health Effects Institute. https://www.healtheffects.org/publication/understanding-health-effects-components-particulate-matter-mix-progress-and-next-steps (accessed 2021-06-27).

(9) Bell, M. L.; HEI Health Review Committee. Assessment of the Health Impacts of Particulate Matter Characteristics. *Res. Rep. Health Eff. Inst.* **2012**, No. 161, 5–38.

(10) West, J. J.; Cohen, A.; Dentener, F.; Brunekreef, B.; Zhu, T.; Armstrong, B.; Bell, M. L.; Brauer, M.; Carmichael, G.; Costa, D. L.; Dockery, D. W.; Kleeman, M.; Krzyzanowski, M.; Künzli, N.; Liousse, C.; Lung, S.-C. C.; Martin, R. V.; Pöschl, U.; Pope, C. A.; Roberts, J. M.;

Russell, A. G.; Wiedinmyer, C. “What We Breathe Impacts Our Health: Improving Understanding of the Link between Air Pollution and Health.” *Environ. Sci. Technol.* **2016**, *50* (10), 4895–4904. https://doi.org/10.1021/acs.est.5b03827.
(11) *Understanding the Health Effects of Ambient Ultrafine Particles*. Health Effects Institute. https://www.healtheffects.org/publication/understanding-health-effects-ambient-ultrafine-particles (accessed 2019-08-13).
(12) Lippmann, M.; Chen, L.-C.; Gordon, T.; Ito, K.; Thurston, G. D. National Particle Component Toxicity (NPACT) Initiative: Integrated Epidemiologic and Toxicologic Studies of the Health Effects of Particulate Matter Components. *Res. Rep. Health Eff. Inst.* **2013**, No. 177, 5–13.
(13) Pond, Z. A.; Hernandez, C. S.; Adams, P. J.; Pandis, S. N.; Garcia, G. R.; Robinson, A. L.; Marshall, J. D.; Burnett, R.; Skyllakou, K.; Garcia Rivera, P.; Karnezi, E.; Coleman, C. J.; Pope, C. A. Cardiopulmonary Mortality and Fine Particulate Air Pollution by Species and Source in a National U.S. Cohort. *Environ. Sci. Technol.* **2022**, *56* (11), 7214–7223. https://doi.org/10.1021/acs.est.1c04176.
(14) Pond, Z. A.; Saha, P. K.; Coleman, C. J.; Presto, A. A.; Robinson, A. L.; Arden Pope III, C. Mortality Risk and Long-Term Exposure to Ultrafine Particles and Primary Fine Particle Components in a National U.S. Cohort. *Environ. Int.* **2022**, *167*, 107439. https://doi.org/10.1016/j.envint.2022.107439.
(15) Krall, J. R.; Chang, H. H.; Sarnat, S. E.; Peng, R. D.; Waller, L. A. Current Methods and Challenges for Epidemiological Studies of the Associations Between Chemical Constituents of Particulate Matter and Health. *Curr. Environ. Health Rep.* **2015**, *2* (4), 388–398. https://doi.org/10.1007/s40572-015-0071-y.
(16) Krewski, D.; Jerrett, M.; Burnett, R. T.; Ma, R.; Hughes, E.; Shi, Y.; Turner, M. C.; Pope, C. A.; Thurston, G.; Calle, E. E.; Thun, M. J.; Beckerman, B.; DeLuca, P.; Finkelstein, N.; Ito, K.; Moore, D. K.; Newbold, K. B.; Ramsay, T.; Ross, Z.; Shin, H.; Tempalski, B. Extended Follow-up and Spatial Analysis of the American Cancer Society Study Linking Particulate Air Pollution and Mortality. *Res. Rep. Health Eff. Inst.* **2009**, No. 140, 5–114; discussion 115-136.
(17) Jerrett, M.; Burnett, R. T.; Ma, R.; Pope, C. A.; Krewski, D.; Newbold, K. B.; Thurston, G.; Shi, Y.; Finkelstein, N.; Calle, E. E.; Thun, M. J. Spatial Analysis of Air Pollution and Mortality in Los Angeles. *Epidemiol. Camb. Mass* **2005**, *16* (6), 727–736. https://doi.org/10.1097/01.ede.0000181630.15826.7d.
(18) Lepeule, J.; Laden, F.; Dockery, D.; Schwartz, J. Chronic Exposure to Fine Particles and Mortality: An Extended Follow-up of the Harvard Six Cities Study from 1974 to 2009. *Environ. Health Perspect.* **2012**, *120* (7), 965–970. https://doi.org/10.1289/ehp.1104660.
(19) Pope, C. A.; Ezzati, M.; Cannon, J. B.; Allen, R. T.; Jerrett, M.; Burnett, R. T. Mortality Risk and PM2.5 Air Pollution in the USA: An Analysis of a National Prospective Cohort. *Air Qual. Atmosphere Health* **2018**, *11* (3), 245–252. https://doi.org/10.1007/s11869-017-0535-3.
(20) Pope, C. A.; Lefler, J. S.; Ezzati, M.; Higbee, J. D.; Marshall, J. D.; Kim, S.-Y.; Bechle, M.; Gilliat, K. S.; Vernon, S. E.; Robinson, A. L.; Burnett, R. T. Mortality Risk and Fine Particulate Air Pollution in a Large, Representative Cohort of U.S. Adults. *Environ. Health Perspect.* **2019**, *127* (7), 77007. https://doi.org/10.1289/EHP4438.
(21) Jerrett, M.; Burnett, R. T.; Beckerman, B. S.; Turner, M. C.; Krewski, D.; Thurston, G.; Martin, R. V.; van Donkelaar, A.; Hughes, E.; Shi, Y.; Gapstur, S. M.; Thun, M. J.; Pope, C. A. Spatial Analysis of Air Pollution and Mortality in California. *Am. J. Respir. Crit. Care Med.* **2013**, *188* (5), 593–599. https://doi.org/10.1164/rccm.201303-0609OC.

(22) Zeger, S. L.; Dominici, F.; McDermott, A.; Samet, J. M. Mortality in the Medicare Population and Chronic Exposure to Fine Particulate Air Pollution in Urban Centers (2000-2005). *Environ. Health Perspect.* **2008**, *116* (12), 1614–1619. https://doi.org/10.1289/ehp.11449.
(23) Apte, J. S.; Messier, K. P.; Gani, S.; Brauer, M.; Kirchstetter, T. W.; Lunden, M. M.; Marshall, J. D.; Portier, C. J.; Vermeulen, R. C. H.; Hamburg, S. P. High-Resolution Air Pollution Mapping with Google Street View Cars: Exploiting Big Data. *Environ. Sci. Technol.* **2017**, *51* (12), 6999–7008. https://doi.org/10.1021/acs.est.7b00891.
(24) Saha, P. K.; Presto, A. A.; Hankey, S.; Murphy, B. N.; Allen, C.; Zhang, W.; Marshall, J. D.; Robinson, A. L. National Exposure Models for Source-Specific Primary Particulate Matter Concentrations Using Aerosol Mass Spectrometry Data. *Environ. Sci. Technol.* **2022**, *56* (20), 14284–14295. https://doi.org/10.1021/acs.est.2c03398.
(25) Wang, Y.; Bechle, M. J.; Kim, S.-Y.; Adams, P. J.; Pandis, S. N.; Pope, C. A.; Robinson, A. L.; Sheppard, L.; Szpiro, A. A.; Marshall, J. D. Spatial Decomposition Analysis of NO2 and PM2.5 Air Pollution in the United States. *Atmos. Environ.* **2020**, *241*, 117470. https://doi.org/10.1016/j.atmosenv.2020.117470.
(26) Pinto, J. P.; Lefohn, A. S.; Shadwick, D. S. Spatial Variability of PM2.5 in Urban Areas in the United States. *J. Air Waste Manag. Assoc.* **2004**, *54* (4), 440–449. https://doi.org/10.1080/10473289.2004.10470919.
(27) Gu, P.; Li, H. Z.; Ye, Q.; Robinson, E. S.; Apte, J. S.; Robinson, A. L.; Presto, A. A. Intracity Variability of Particulate Matter Exposure Is Driven by Carbonaceous Sources and Correlated with Land-Use Variables. *Environ. Sci. Technol.* **2018**, *52* (20), 11545–11554. https://doi.org/10.1021/acs.est.8b03833.
(28) Sun, Y.-L.; Zhang, Q.; Schwab, J. J.; Demerjian, K. L.; Chen, W.-N.; Bae, M.-S.; Hung, H.-M.; Hogrefe, O.; Frank, B.; Rattigan, O. V.; Lin, Y.-C. Characterization of the Sources and Processes of Organic and Inorganic Aerosols in New York City with a High-Resolution Time-of-Flight Aerosol Mass Apectrometer. *Atmospheric Chem. Phys.* **2011**, *11* (4), 1581–1602. https://doi.org/10.5194/acp-11-1581-2011.
(29) Ulbrich, I. M.; Canagaratna, M. R.; Zhang, Q.; Worsnop, D. R.; Jimenez, J. L. Interpretation of Organic Components from Positive Matrix Factorization of Aerosol Mass Spectrometric Data. *Atmospheric Chem. Phys.* **2009**, *9* (9), 2891–2918. https://doi.org/10.5194/acp-9-2891-2009.
(30) Eeftens, M.; Beelen, R.; de Hoogh, K.; Bellander, T.; Cesaroni, G.; Cirach, M.; Declercq, C.; Dėdelė, A.; Dons, E.; de Nazelle, A.; Dimakopoulou, K.; Eriksen, K.; Falq, G.; Fischer, P.; Galassi, C.; Gražulevičienė, R.; Heinrich, J.; Hoffmann, B.; Jerrett, M.; Keidel, D.; Korek, M.; Lanki, T.; Lindley, S.; Madsen, C.; Mölter, A.; Nádor, G.; Nieuwenhuijsen, M.; Nonnemacher, M.; Pedeli, X.; Raaschou-Nielsen, O.; Patelarou, E.; Quass, U.; Ranzi, A.; Schindler, C.; Stempfelet, M.; Stephanou, E.; Sugiri, D.; Tsai, M.-Y.; Yli-Tuomi, T.; Varró, M. J.; Vienneau, D.; Klot, S. von; Wolf, K.; Brunekreef, B.; Hoek, G. Development of Land Use Regression Models for PM2.5, PM2.5 Absorbance, PM10 and PMcoarse in 20 European Study Areas; Results of the ESCAPE Project. *Environ. Sci. Technol.* **2012**, *46* (20), 11195–11205. https://doi.org/10.1021/es301948k.
(31) Saha, P. K.; Li, H. Z.; Apte, J. S.; Robinson, A. L.; Presto, A. A. Urban Ultrafine Particle Exposure Assessment with Land-Use Regression: Influence of Sampling Strategy. *Environ. Sci. Technol.* **2019**, *53* (13), 7326–7336. https://doi.org/10.1021/acs.est.9b02086.
(32) US EPA, O. *2017 National Emissions Inventory (NEI) Data*. https://www.epa.gov/air-emissions-inventories/2017-national-emissions-inventory-nei-data (accessed 2022-12-01).

(33) Zhang, Q.; Jimenez, J. L.; Canagaratna, M. R.; Ulbrich, I. M.; Ng, N. L.; Worsnop, D. R.; Sun, Y. Understanding Atmospheric Organic Aerosols via Factor Analysis of Aerosol Mass Spectrometry: A Review. *Anal. Bioanal. Chem.* **2011**, *401* (10), 3045–3067. https://doi.org/10.1007/s00216-011-5355-y.
(34) Shah, R. U.; Robinson, E. S.; Gu, P.; Robinson, A. L.; Apte, J. S.; Presto, A. A. High-Spatial-Resolution Mapping and Source Apportionment of Aerosol Composition in Oakland, California, Using Mobile Aerosol Mass Spectrometry. *Atmospheric Chem. Phys.* **2018**, *18* (22), 16325–16344. https://doi.org/10.5194/acp-18-16325-2018.
(35) Lim, H.-J.; Turpin, B. J. Origins of Primary and Secondary Organic Aerosol in Atlanta: Results of Time-Resolved Measurements during the Atlanta Supersite Experiment. *Environ. Sci. Technol.* **2002**, *36* (21), 4489–4496. https://doi.org/10.1021/es0206487.
(36) Zhao, Y.; Tkacik, D. S.; May, A. A.; Donahue, N. M.; Robinson, A. L. Mobile Sources Are Still an Important Source of Secondary Organic Aerosol and Fine Particulate Matter in the Los Angeles Region. *Environ. Sci. Technol.* **2022**, *56* (22), 15328–15336. https://doi.org/10.1021/acs.est.2c03317.
(37) Aiken, A. C.; DeCarlo, P. F.; Kroll, J. H.; Worsnop, D. R.; Huffman, J. A.; Docherty, K. S.; Ulbrich, I. M.; Mohr, C.; Kimmel, J. R.; Sueper, D.; Sun, Y.; Zhang, Q.; Trimborn, A.; Northway, M.; Ziemann, P. J.; Canagaratna, M. R.; Onasch, T. B.; Alfarra, M. R.; Prevot, A. S. H.; Dommen, J.; Duplissy, J.; Metzger, A.; Baltensperger, U.; Jimenez, J. L. O/C and OM/OC Ratios of Primary, Secondary, and Ambient Organic Aerosols with High-Resolution Time-of-Flight Aerosol Mass Spectrometry. *Environ. Sci. Technol.* **2008**, *42* (12), 4478–4485. https://doi.org/10.1021/es703009q.
(38) Hayes, P. L.; Ortega, A. M.; Cubison, M. J.; Froyd, K. D.; Zhao, Y.; Cliff, S. S.; Hu, W. W.; Toohey, D. W.; Flynn, J. H.; Lefer, B. L.; Grossberg, N.; Alvarez, S.; Rappenglück, B.; Taylor, J. W.; Allan, J. D.; Holloway, J. S.; Gilman, J. B.; Kuster, W. C.; Gouw, J. A. de; Massoli, P.; Zhang, X.; Liu, J.; Weber, R. J.; Corrigan, A. L.; Russell, L. M.; Isaacman, G.; Worton, D. R.; Kreisberg, N. M.; Goldstein, A. H.; Thalman, R.; Waxman, E. M.; Volkamer, R.; Lin, Y. H.; Surratt, J. D.; Kleindienst, T. E.; Offenberg, J. H.; Dusanter, S.; Griffith, S.; Stevens, P. S.; Brioude, J.; Angevine, W. M.; Jimenez, J. L. Organic Aerosol Composition and Sources in Pasadena, California, during the 2010 CalNex Campaign. *J. Geophys. Res. Atmospheres* **2013**, *118* (16), 9233–9257. https://doi.org/10.1002/jgrd.50530.
(39) Kim, S.-Y.; Bechle, M.; Hankey, S.; Sheppard, L.; Szpiro, A. A.; Marshall, J. D. Concentrations of Criteria Pollutants in the Contiguous U.S., 1979 – 2015: Role of Prediction Model Parsimony in Integrated Empirical Geographic Regression. *PLOS ONE* **2020**, *15* (2), e0228535. https://doi.org/10.1371/journal.pone.0228535.
(40) Habre, R.; Girguis, M.; Urman, R.; Fruin, S.; Lurmann, F.; Shafer, M.; Gorski, P.; Franklin, M.; McConnell, R.; Avol, E.; Gilliland, F. Contribution of Tailpipe and Non-Tailpipe Traffic Sources to Quasi-Ultrafine, Fine and Coarse Particulate Matter in Southern California. *J. Air Waste Manag. Assoc.* **2021**, *71* (2), 209–230. https://doi.org/10.1080/10962247.2020.1826366.
(41) Fussell, J. C.; Franklin, M.; Green, D. C.; Gustafsson, M.; Harrison, R. M.; Hicks, W.; Kelly, F. J.; Kishta, F.; Miller, M. R.; Mudway, I. S.; Oroumiyeh, F.; Selley, L.; Wang, M.; Zhu, Y. A Review of Road Traffic-Derived Non-Exhaust Particles: Emissions, Physicochemical Characteristics, Health Risks, and Mitigation Measures. *Environ. Sci. Technol.* **2022**, *56* (11), 6813–6835. https://doi.org/10.1021/acs.est.2c01072.

(42) Wang, X.; Gronstal, S.; Lopez, B.; Jung, H.; Chen, L.-W. A.; Wu, G.; Ho, S. S. H.; Chow, J. C.; Watson, J. G.; Yao, Q.; Yoon, S. Evidence of Non-Tailpipe Emission Contributions to PM2.5 and PM10 near Southern California Highways. *Environ. Pollut.* **2023**, *317*, 120691. https://doi.org/10.1016/j.envpol.2022.120691.
(43) Goldstein, A. H.; Koven, C. D.; Heald, C. L.; Fung, I. Y. Biogenic Carbon and Anthropogenic Pollutants Combine to Form a Cooling Haze over the Southeastern United States. *Proc. Natl. Acad. Sci.* **2009**, *106* (22), 8835–8840. https://doi.org/10.1073/pnas.0904128106.

Supplemental Material

Supplementary material are available online. All the LUR model estimates are publicly available at https://www.caces.us/

Acknowledgments

This research is part of the Center for Air, Climate, and Energy Solutions (CACES), which was supported by the Environmental Protection Agency (assistance agreement number RD83587301). It has not been formally reviewed by EPA. The views expressed in this document are solely those of authors and do not necessarily reflect those of the Agency. EPA does not endorse any products or commercial services mentioned in this publication.